Experiments in vortex avalanches

E. Altshuler[*]

Superconductivity Laboratory and "Henri Poincaré" Group of Complex Systems, IMRE–Physics Faculty, University of Havana, 10400 Havana, Cuba

T. H. Johansen[†]

Department of Physics, University of Oslo, Blindern, N-0316 Oslo, Norway

(Dated: March 22, 2024)

Avalanche dynamics is found in many phenomena spanning from earthquakes to the evolution of species. It can be also found in vortex matter when a type II superconductor is externally driven, for example, by increasing the magnetic field. Vortex avalanches associated with thermal instabilities can be an undesirable effect for applications, but "dynamically driven" avalanches emerging from the competition between intervortex interactions and quenched disorder constitute an interesting scenario to test theoretical ideas related with non-equilibrium dynamics. However, differently from the equilibrium phases of vortex matter in type II superconductors, the study of the corresponding dynamical phases –in which avalanches can play a role– is still in its infancy. In this paper we critically review relevant experiments performed in the last decade or so, emphasizing the ability of different experimental techniques to establish the nature and statistical properties of the observed avalanche behavior.

Contents

I. INTRODUCTION

Rooted somewhere between Physics and Engineering, the critical state model of Charles P. Bean (1962) continues to enjoy an immense popularity amongst those who need to understand the magnetic properties of almost all potentially useful superconductors. Above a certain magnetic field threshold, type II superconductors are penetrated by superconducting vortices, or flux lines, each one consisting in a normal-state core surrounded by a tiny supercurrent tornado with a few-dozen-nanometer radius. The vortices can therefore be thought of as long and thin solenoid magnets which enter into the sample in increasing numbers as the external field grows. In a perfect superconducting crystal, the competition between the inter-vortex repulsion and the "magnetic pressure" from the outside field causes the vortices to arrange in a hexagonal lattice (Abrikosov, 1957). In a real superconductor, however, there are defects acting as pinning centers, and the vortex motion becomes impeded. The interplay of all these forces, where an external drive "pushing in" more and more vortices is counteracted by pinning, results in a non-equilibrium state, the critical state, with a vortex density being largest near the surfaces where flux enters the sample. This critical state typically involves several million vortices, and as the external field is increased or decreased, they readily find the way to organize themselves in spite of their short range interactions. Researchers in the area of Complexity would not hesitate these days in characterizing Bean's critical state as an emergent phenomenon resulting from the self organization of a complex system of vortices.

But those are not empty words. They call attention to the fact that the collective, nonlinear statistical properties of a complex system can produce amazing macroscopic results, regardless of the details of the interaction between their microscopic constituents. They also suggest that we should open up our mind and try to find analogies in eventually very distant fields of science. After all, isn't a sandpile a quite good analogue of Bean's critical state? As grains are added to a sandpile from the top, gravity tries to bring them off the pile, a motion which is prevented by the intergrain friction. And again, in spite of the short range character of the latter, the pile finds the way to organize itself and produce globally an angle of repose, or critical angle. In very simple terms, you can identify the gravity as the magnetic field applied to superconductors, while friction corresponds to vortex

[*]Electronic address: jea@infomed.sld.cu
[†]Electronic address: t.h.johansen@fys.uio.no

pinning. This would have sounded like celestial music in the ears of Lord Kelvin, who once wrote "I am never content until I have constructed a mechanical model of the subject I am studying. If I succeed in making one, I understand; otherwise I do not." (Kelvin, 1884).

Grasping the analogy between the critical state and the sandpile well before the era of Complexity ideas, Pierre G. De Gennes expresses in his classic 1966 book Superconductivity of Metals and Alloys: "We can get some physical feeling of this critical state by thinking of a sand hill. If the slope of the sand hill exceeds some critical value, the sand starts flowing downwards (avalanche). The analogy is, in fact, rather good since it has been shown (by careful experiments with pickup coils) that, when the system becomes over-critical, the lines do not move as single units, but rather in the form of avalanches including typically 50 lines or more" (De Gennes, 1966). This picture was dormant for many years until scientists working in the field of Complexity identified avalanche dynamics as a major mechanism in many physical, chemical, biological and social phenomena. In particular, the ideas of Self Organized Criticality (SOC) find avalanches with "robust" power-law distributions of sizes and durations, at the core of the underlying dynamics in many systems (Bak, 1996; Jensen, 1998). With the sandpile being a central paradigm of SOC theory, Bean's critical state has become a natural playground to look for avalanche dynamics. Although heroic efforts were made in the 1960s to see these avalanches, it was computer-controlled data acquisition that made it possible to investigate vortex avalanche statistics in superconductors. Other advances such as micro Hall probes and high resolution magneto-optical imaging have finally stamped the seal of contemporary times on these studies. "Dynamically driven" avalanches like the ones suggested by the sandpile analogy can, after all, be the intrinsic mechanism in the formation of the critical state that Charles P. Bean would have never dreamed of.

In Bean's time, however, another kind of vortex avalanche attracted most of the attention: flux jumps. Instead of helping to establish the critical state, they tend to destroy it, producing undesirable jumps in the sample magnetization. In contrast to the avalanches discussed in connection with sandpiles, flux jumps are thermally triggered. If the external field is increased too fast, and the thermal capacity and conductivity of the sample are small, the vortices rushing in will dissipate heat due to their motion, and the local temperature rises. This tends to detach other vortices from their pinning sites, leading to new motion that can cause even further heating. This positive feedback process may sweep away the critical state in a big region of the sample, and translates into a sudden, catastrophic decrease in the magnetization. Thermally triggered avalanches have long been modeled in terms of macroscopic parameters. However, present imaging techniques have provided data showing that these events sometimes also result in complex magnetic spatial structures which deserve a more detailed explanation.

All of these findings suggest that the simple sandpile analogy of vortex avalanches must be examined with caution: For one thing, temperature is not accounted for in the standard SOC picture. At this point, many questions arise: Can experiments reveal a sharp difference between dynamically and thermally driven avalanches? If so, can we through statistical analyses of the dynamically driven avalanches conclude whether Bean's critical state model represents an SOC phenomenon? What is the relation between the details of the magnetic flux distribution inside the sample and the avalanche dynamics? Some authors have directly aimed their experimental efforts at these subjects. Others offer relevant data just as experimental "side effects." The fairly few available outputs can be characterized as diverse and entangled, and it is the purpose of this Colloquium is to provide a coherent overview that highlights the essence of the results obtained in this area during the last decade or so.

II. THE NATURE OF VORTEX AVALANCHES

A. The critical state

When the external magnetic field exceeds the so-called lower critical field, H_{c1}, the surface layer of a type-II superconductor starts to give birth to vortices, which immediately are pushed deeper into the material by the Meissner shielding currents. Each flux line consists of a "normal" core of radius ξ, the coherence length, surrounded by a circulating supercurrent decaying over a distance λ, the London penetration depth. The current is accompanied by an axial magnetic field decaying over the same λ, and integrates to a total amount of flux equal to the flux quantum $\Phi_0 = h/2e \approx 2 \times 10^{-15}$ Tm^2, where h is Planck's constant and e is the elementary charge. As the applied field keeps increasing, the vortices get closer and closer until the overlapping is so heavy, that an overall transition to the normal state takes place at the upper critical field, H_{c2}. When microscopic defects are present in the material, such areas tend to pin any vortex that passes by. The pinning force always acts against the driving force, which on a vortex has a Lorentz-like form, $f_L = J \times \Phi_0 \hat{z}$, where J is the local density of either a transport current or a magnetization current (Meissner current and/or gradients in the number of neighboring vortices), or both. The basic assumption of the critical state model is that as the vortices invade the sample, every pinning center that catches a vortex will hold onto it as hard as it possibly can, quantified by a certain maximum pinning force per unit vortex length, f_p^{max}. In this way the local balance between the two competing forces, $|f_L| = f_p^{max}$, creates a metastable equilibrium state, where the current density adjusts itself to a maximum magnitude, $|J^{max}| \equiv J_c$, the critical current density. From Ampere's law it then follows that the flux density distribution, $B(r)$, in the

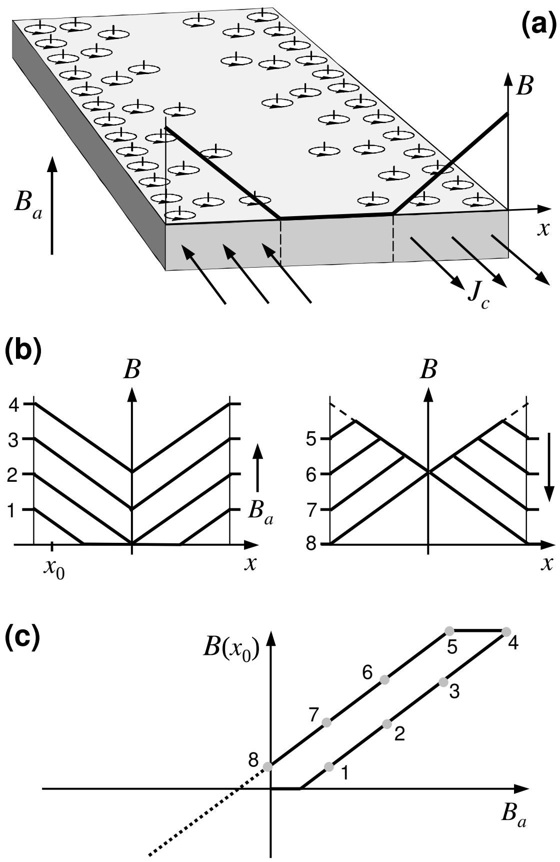

FIG. 1 Bean's critical state; (a) the distribution of vortices, internal field and current in a superconductor placed in an external magnetic field, B_a. (b) internal field profiles for increasing (left) and decreasing (right) B_a, and (c) variation of the local field at x_0 during the cycle in (b).

critical state is given by

$$|\nabla \times \mathbf{B}(\mathbf{r})| = \mu_0 J_c . \qquad (1)$$

The vortices therefore organize in such a way that their density decreases linearly from the edges of the sample, and the slope is $\mu_0 J_c$, as illustrated in Fig. 1(a). Shown in Fig. 1(b) is a set of B-profiles that occur at different stages during an ascent (left) and the subsequent descent (right) of the applied field. From the illustration it is evident that this strongly hysteretic process is quite analogous to what happens to a box of sand where sand is first added near the side walls (left), and afterwards the walls are gradually lowered to zero height (right). The crux is then: How do such systems evolve in space and time as they are driven externally through a "continuous sequence" of different critical states?

B. Dynamically and thermally driven avalanches

The idea of dynamically driven avalanches in the vortex matter relates to one possible way for the system to respond when subjected to a slow drive, e.g., a gentle ramping of the applied magnetic field. By driving the vortices sufficiently slowly only their mutual repulsion and the interactions with pinning sites are expected to control the dynamics. If SOC provides the correct description, the critical state behavior should show scale invariant avalanche dynamics, i.e., the distribution of avalanche sizes follows a power law, $P(s) \propto s^{-\tau}$. Here $P(s)$ is the probability to find an avalanche event where s vortices suddenly move, and τ is a critical exponent. While in the original formulation of SOC the exponent $\tau \approx 1$ is found to be robust with respect to small changes in the model, later developments of the theory have shown that the exponent can vary within a certain range.

Note that in some cases the finding of temporal signals exhibiting scaling, e.g., signals with $1/f$ noise in the power spectrum, has been taken as direct evidence for SOC behavior. However, observation of $1/f$ noise should not be considered a sufficient indication of SOC, since it can result even from a spread of activation energies (Jensen, 1998; O'Brien and Weissman, 1992).

Whether real piles follow the SOC scheme is still subject to debate (Altshuler et al., 1999; Bretz et al., 1992; Frette et al., 1996; Held et al., 1990; Rosendahl et al., 1993, 1994), and a similar discussion extends also to several other systems (D'Anna and Nori, 2000; Field et al., 1995; Plourde et al., 1993). It is therefore important to note that the critical state of type II superconductors represents a unique and attractive case to study. In contrast to grains of sand, the vortices are non-inertial objects, and are hence closer to the idealized formulation of the SOC theory.

As in most areas where SOC ideas have been applied, the theoretical papers largely outnumber the experimental studies of vortex avalanches. Let us therefore, as a background for the main part of this Colloquium, mention briefly the important trends in the theoretical work, emphasizing ideas and results that most directly connect to the available experiments. Among computer simulation there are two philosophies dominating the literature; molecular dynamics (MD) and cellular automata (CA). In addition, a few reports using a macroscopic approach have been published.

Most macroscopic treatments discuss vortex avalanches in a thermal activation scenario (Bonabeau and Lederer, 1995, 1996; Pan and Doniach, 1994; Prozorov and Giller, 1999; Tang, 1993; Vinokur et al., 1991). Although some of these authors claim to find fingerprints of SOC behavior, their results are not compatible with the "canonical" formulation by Bak et al. (1987): As in a shaking sandpile, thermal activation makes the critical state to relax away from the marginal stability because vortices, or bundles of them, jump out of their pinning centers, and redistribute in such a way that the Bean's profile changes in time. This phenomenon, known as flux creep, was first observed by Kim et al. in 1963, and its typical manifestation is a slow, logarithmic temporal decay of the magnetization

(Yeshurun, 1996). Thus, flux creep can only be allowed within a "soft" definition of SOC, eventually useful to interpret certain relaxation experiments which will be discussed later in this Colloquium ((Aegerter, 1998)). There are also macroscopic studies that do ignore flux creep effects (Barford, 1997). Here, the author proposes an equation of motion to analyze the dynamics of the critical state as the external field is increased, and finds a power law in the distribution of avalanche sizes with a critical exponent of 1.13, consistent with the original SOC picture.

Typical for the MD simulations is that they allow integration of the equations of motion at the vortex level. Since this demands quite high computing power, the MD work deals mostly with small systems. The CA approach, on the other hand, simplifies the dynamics by selecting a set of physically sound rules that imitate the real laws, thereby allowing simulation of much bigger systems. Care must be taken, however, since the results can be sensitive to the selected set of rules (see, for example, Kadanoff et al. (1989)).

After the pioneering application of MD techniques in the investigation of vortex avalanches in the critical state by Richardson et al. (1994), extensive work on the subject has been generated (Barford et al., 1993; Olson et al., 1997,a; Pla et al., 1996). A MD simulation of a slowly driven critical state can be illustrated by the approach of Olson et al. (1997): For every vortex, i, they solve the overdamped equation of motion

$$f_i = f_i^{vv} + f_i^{vp} = \eta v_i , \qquad (2)$$

where f_i is the total force, comprised of f_i^{vv} – the inter-vortex repulsion, and f_i^{vp} – the interaction between the vortex and a pinning center. The v_i is the vortex velocity, and η the "viscosity" of vortex flow. With this realistic description of each member of the ensemble the simulations show that a critical state flux profile builds up when vortices are slowly added from one side of the "sample". If one keeps adding vortices after the critical state is fully established, their effect can be followed by calculating the time evolution of the average vortex velocity. Typically, this shows bursts of activity, or avalanches, which resemble the voltage signals found in the pick up experiments discussed below (Field et al., 1995). The avalanche size distribution resulting from these simulations follows a power law. When counting all the moving vortices for each avalanche event, one finds an exponent in the range $0.9 - 1.4$, where the spread comes from varying the strength and density of the pinning sites. Similarly, for off-the-edge avalanches (counting only the number of vortices exiting through the "sample edge" during an event) one finds $2.4 - 4.4$. Although these distributions are often well-behaved over quite a broad range, it is also clear that the exponent is not very robust.

The CA approach was introduced in a model by Bassler and Paczuski (1998), where they considered vortex dynamics on a two-dimensional honeycomb lattice (see Fig. 2). Each cell x, which has three nearest neighbors, is

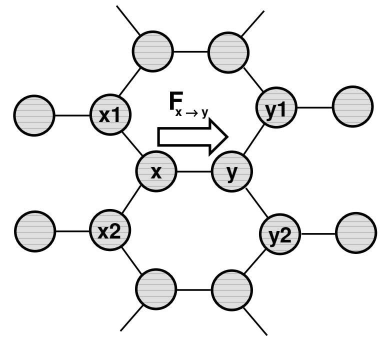

FIG. 2 Site lattice illustrating the Bassler-Paczuski cellular automata used for modelling vortex avalanches (Bassler and Paczuski, 1998).

occupied by an integer number of vortices. The authors then assume that force pushing a vortex at x towards the neighbor cell y consists of two basic contributions: Firstly, to mimic the vortex-vortex repulsion the force increases as the population at x gets bigger than that at y. A similar term representing the next nearest neighbor repulsion is also included. Secondly, to simulate the vortex-pin attraction, the force increases as the pinning potential of y is bigger x (the pinning potential is represented by a random number assigned to each cell). In each time step, the cells are updated in parallel; a vortex moves to a neighboring cell if the force in that direction is positive. If a vortex is attracted in more than one direction, the selection can be made at random (Bassler and Paczuski, 1998) or by a largest force rule (Bassler et al., 2001). When vortices are now added at one edge of the "sample," this CA leads to a critical state very close to the ideal Bean's flux profile. As in the MD simulations, one finds here avalanche dynamics, and the size distribution of avalanches was reported to have a critical exponent of 1.63 ± 0.02 (obtained after finite size scaling for four orders of magnitude in avalanche size). In contrast to the MD work, the exponent is here essentially constant within the range of parameters studied, therefore suggesting a SOC scenario (Bassler and Paczuski, 1998). The application of the model to the case of periodic, dense pinning, indicates a slight decrease in the exponent to 1.45 ± 0.02 (Cruz et al., 2000).

Besides SOC there are also other theories producing power laws in the avalanche size distributions (Carlson and Doyle, 1999; Huang et al., 1997; Newman and Sneppen, 1996; Schwarz and Fisher, 2001). Among these, the model of Newman and Sneppen (1996) seems the most relevant to the critical state, although the excitation in the form of "coherent noise" is not obviously applicable to vortex dynamics.

Catastrophic avalanches – flux jumps – are associated with a "runaway" in the motion of vortices as they redistribute in response to e.g. an increasing applied field. Per unit volume, the motion generates heat at the rate of $J_c E$, where E is the electrical field. Due to this dissipation, the critical current density and thereby the shielding goes down, and more vortices rush into the sample. This positive feedback may or may not result in a flux jump. The superconductor is stable if the heat dissipation does not exceed the material's ability to store heat, a criterion that under adiabatic conditions can be expressed as (Mints and Rakhmanov, 1981)

$$\beta = \frac{\mu_0 J_c(T) w^2}{c} \left|\frac{dJ_c}{dT}\right| < 1 , \tag{3}$$

where c is the specific heat, and w a typical dimension of the sample.[1] However, if $\beta > 1$, flux jumps are to be expected, and the first jump will occur when the field reaches the value $B_{fj} \approx \sqrt{\mu_0 c (T_c - T)}$. Here T_c is the critical temperature, and a linear $J_c(T)$ is assumed as a reasonable approximation. Let us put numbers on two cases that will be discussed later. For the 1.5×1.5 mm^2-area Nb foils used in Altshuler et al. (2002), one gets $\beta \approx 5 \times 10^{-3}$, so flux jumps at the temperature of 4.6 K can be discarded. For the mm-sized YBaCuO crystals studied in the sub-Kelvin range by Seidler et al. (1993) and Zieve et al. (1996), β becomes close to 3, and the situation is marginal. If flux jumps were to take place, they would here start at $B_{fj} \approx 5$ Tesla, actually not very far from the threshold fields reported by these authors. However, estimates like these must be seen with caution. No real experiment takes place under ideal adiabatic conditions, so other factors need to be considered as well. Generally, the "recipe" to avoid flux jumps is to choose samples with high thermal conductivity, make sure that their thermal contact with the environment is good, and be gentle when ramping the applied field.

III. EXPERIMENTAL TECHNIQUES

The various magnetometric techniques used to measure vortex avalanches can be classified as global and local. The global techniques are sensitive to either the amount of flux passing through the surface of the sample or the volume averaged magnetic moment, whereas the local techniques are detecting the flux density or even the individual vortex positions in selected regions. In this section we give a brief overview of the various methods used in these experiments.

Pick up coil detection is the most basic global technique, and is typically configured as a coil wound tightly around the sample. When the external field is ramped up or down, the magnetic flux that enters or leaves the sample will (according to Faraday's law) induce a voltage in the coil proportional to the rate of this "traffic" of vortices. Therefore, a steady-state flux motion results in a constant voltage output, while the appearance of spikes in the signal implies step-like increments, i.e., vortex avalanche events. By integrating the voltage in time one can determine, at least approximately, also the amount of flux involved in such events, as done in the careful experiments of Field et al., described in more detail below.

Another important technique is Superconducting Quantum Interference Device (SQUID) magnetometry (Barone and Paterno, 1982). The basic sensor here is a closed superconducting loop interrupted by, for instance, two Josephson junctions. A dc bias current is injected in such a way that it flows through the two junctions in parallel. If the loop is now subjected to a magnetic field, this produces a shift of the superconducting phase difference through the junctions, analogous to the phase difference between the various optical paths in the Young's double slit experiment. As a consequence, the maximum bias current that can be forced into the SQUID without dissipation becomes field dependent: $i_m(\Phi_{ext}) = 2I_{cj}|\cos(\pi\Phi_{ext}/\Phi_0)|$, where I_{cj} is the Josephson critical current of each junction, and Φ_{ext} is the magnetic flux threading the SQUID loop. The periodic form of i_m implies that such a sensor can "intrinsically detect" magnetic flux with a resolution of less than one flux quantum Φ_0. In practice, the field sensitivity of the SQUID depends on the loop area, and on the design of flux transformers. The areas of SQUID loops (or flux transformer pick up coils) typically span from around 1 mm^2 to 0.04 mm^2 (Lee et al., 1995), the latter making it possible to apply the device for local measurements.

While sensors based on the Hall effect have long since proved very powerful, it was the invention of the modulation-doped semiconductor heterostructure (Dingle et al., 1978) that gave rise to the present state-of-the-art sensors, the micro-Hall probes. These epitaxial structures, mostly GaAl/AlGaAs, consist of 2D layers of electrons with large carrier mobilities at low temperatures. The active area of the sensing element spans from 100 μm^2 to less than 1 μm^2. Note then that if just one flux quantum Φ_0 is present under a 100 μm^2 probe, the effective field is ≈ 0.2 Oe. Typically, this produces a Hall output of 2 μV for a bias current of 100 μA. Micro-Hall probes can today be manufactured also as arrays of sensors in either linear or matrix arrangements. A practical linear array is composed of 11 square probes of 100 μm^2 each, separated by 20 μm center-to-center (Altshuler et al., 2002). Micro Hall probes can also be attached to a piezoelectric scanner tube (as in a tunneling microscope) forming a scanning Hall probe microscope (SHM) (Bending, 1999). Such a device is able to magnetically scan the sample with sub-micron spatial resolution, and resolve the field from individual vortices. A limitation of the method is that a standard SHM can scan only small areas, typically 25×25 μm^2 at 77 K (Oral et al., 1996).

The only technique which today allows experiments with combined high spatial and temporal resolution is magneto-optical imaging (MOI). Here the sensing element is a strongly Faraday rotating film, which one places directly on top of the sample under investigation. As

[1] A prefactor of order unity is omitted in the formula.

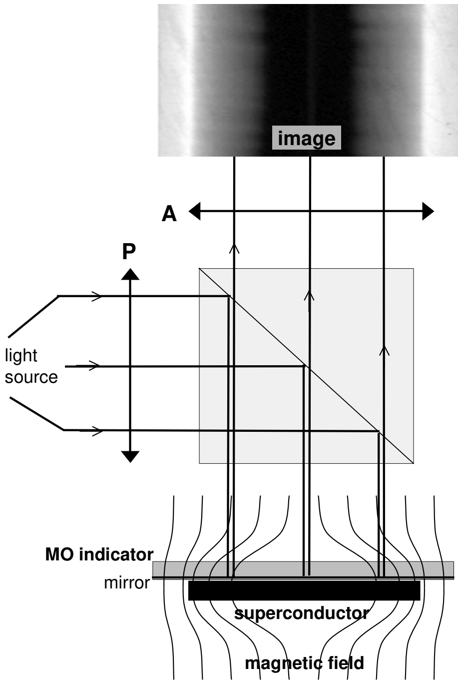

FIG. 3 Principle of the magneto-optical imaging (MOI) technique. A magneto-optical indicator film placed on top of the superconductor gives the incoming polarized light a Faraday rotation according to the local magnetic field. After being reflected and passed through a crossed analyzer, the light produces an image in which the intensity contrast is a direct map of the field distribution.

illustrated in Fig. 3 the imaging is done by shining polarized light through the film, where reflection from a mirror, or the sample itself, gives the light a second pass that doubles the Faraday effect. The light contains then a distribution of rotation angles, θ_F, corresponding to the magnetic field variations across the face of the superconductor. Finally, an analyzer set at 90° crossing relative to the polarizer filters the light and produces an optical image where the brightness shows directly how the magnetic field was distributed. Since MOI was invented in the 1950s several materials have been used as indicator films (Koblischka and Wijngaarden, 1995). During the last decade the most popular material by far has been the in-plane magnetization ferrite garnet films, often $(Lu,Bi)_3(Fe,Ga)_5O_{12}$, grown as a few micron thick epitaxial layer on gadolinium gallium garnet (transparent) substrates. The sensitivity of these indicators is represented by the low-field Verdet constant, $V = \theta_F/Hd$, where d is the film thickness. For green light (strongly present in Hg-lamps) one has $V \simeq 2-8$ degrees/kOe per micron, which is sufficient to resolve individual vortices (Goa et al., 2001). The unique power of the MOI technique is two-fold; first, by simple optical means one may zoom between cm- and micron-sized fields-of-view, and second, the time response of the garnet film is extremely fast, of the order of nanoseconds (Runge et al., 2000).

IV. REVIEW OF RECENT EXPERIMENTS

A. Pick up coil experiments

The first experiment on vortex avalanches inspired by the SOC ideas was reported by Field and coworkers in 1995 (Field et al., 1995). An 1800 turn pickup coil was coaxially mounted on the inner surface of a tube made from the conventional superconductor NbTi. The tube had a 6 mm outer diameter, a wall thickness of 0.25 mm and it was 3.4 cm long, nearly twice the length of the pickup coil. As noted by Field et al. (1995), this geometry guarantees a close analogy to (conical) sandpiles. An external magnetic field was applied along the tube axis at various ramp speeds, and the voltage induced in the pickup coil was amplified and recorded by a computer. The upper section of Fig. 4 displays the time variation of the signal over a field interval of 30 Oe centered at 7.55 kOe using the fairly low ramp rate of 5 Oe/s.[2] The authors identify two contributions to the flux penetration: A first one, amounting to about 97 % of the flux, corresponds to the background level, and is believed to represent the thermally activated "smooth" flow of vortices. The second contribution is the well-defined spikes, which clearly indicate the presence of flux avalanches.

The lower panel of the figure shows the avalanche size distributions obtained from such experiments performed at 3 different fields. In all the cases the distribution follows a nice power law over more than one decade. The observed non-monotonous change in the exponent from -1.4 to -2.2 is attributed by Field and coworkers to the different inter-vortex distances attained at the various fields. This may be considered analogous to the influence of grain friction, shape (Frette et al., 1996) and also type of base (Altshuler et al., 1999) on the similar exponents describing sandpile dynamics. The authors also report "$1/f$" noise in their experiments, finding power laws for low enough field ramp rates.

Let us take a closer look at how the avalanche size was determined in the work of Field et al. (1995). Consider a flux avalanche of length l – the length along the tube where a set of vortices "drops" out of the superconductor and spills into the hole where the coil is located. Only the corresponding number of turns, $n = lN/L$, where L and N are the coil's total length and number of turns, respectively, will pick up the flux change, and the coil responds by inducing the voltage $V = n(d\Phi/dt)$, where $\Phi = \mathcal{N}\Phi_0$ is the number of vortices participating in the event. From this the authors defined the avalanche size as an "effective bundle volume" given by $s \equiv l\mathcal{N} = (L/N)\int V\,dt$. This is a convenient definition since it was not possible

[2] An accepted experimental meaning of a ramp rate being sufficiently low in the search for SOC behavior, is that the resulting avalanche statistics becomes insensitive to the actual chosen rate. Typically, this occurs below 10 Oe/s.

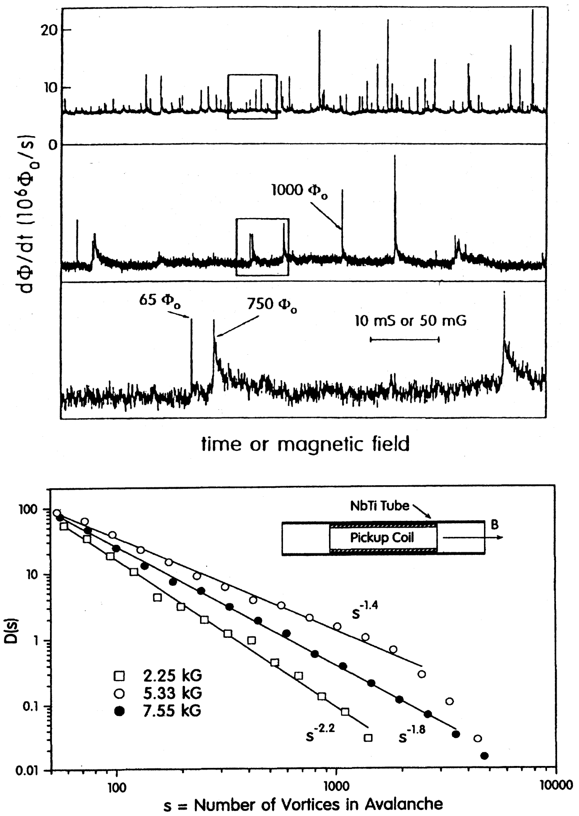

FIG. 4 Vortex avalanches reported by Field et al. (1995). Upper group of three panels: voltage output for different time windows, at a field window centered at 7.55 kOe. Note that the data shown in the small frames in the first and second panels are shown on an expanded scale in the second and third panels, respectively. Lower Panel: avalanche size distributions for different field windows. The inset in this panel shows the experimental arrangement.

to determine l directly from the measurements.[3]

We suggest that the avalanche length l can be estimated using the collective pinning theory (Larkin and Ovchinnikov, 1973, 1979). According to it, the elastically deformed vortex lattice is characterized by the length L_c^b and R_c along, and normal, to the field direction, respectively (Blatter et al., 1991, 1994). Over this volume the vortices are collectively pinned and behave essentially as one bundle. The value of l can be evaluated through the simple formula $l \approx L_c^b \approx (\ ^2\ ^3/a_0^4)(J_0/J_c)^{3/2}$, where a_0 is the inter-vortex distance and J_0 is the depairing current density (, and J_c are defined in section II.A). Substituting typical numbers for a low-T_c alloy at temperatures below 5 K (Campbell and Evetts, 1972), with a_0 corresponding to a few kOe field, we get an L_c^b of a few hundred microns (Altshuler, 2001), i.e., much smaller than the length of the pickup coil. Interestingly, a very early experiment by Wischmeyer (Wischmeyer et al., 1967), where two separate coils – both similar to the one used by Field et al. – were mounted one after the other on the inside of a Nb tube, gave two more or less uncorrelated signals. The two coils were separated by a gap of 2.5 mm, supporting the above estimate for the size of the "avalanching objects."

In spite of the limitations inherent in the method used by Field et al. (1995), this paper critically fueled much of the studies of dynamically driven vortex avalanches in the second half of the 1990s.

B. Micro Hall probe experiments

In contrast to the pick up coil technique, Hall probes allow one to directly measure the size of the "avalanching object" in flux units. An avalanche event appears here as an abrupt step in the Hall signal, and the size of the step represents the change in the number of vortices populating the area under the probe. Such experiments were first done by Seidler et al. (1993), who with a $2 \times 10\ \mu m^2$ area Hall probe detected avalanches in 70 μm thick, untwinned YBaCuO crystals during field ramps at 8 Oe/s. The measurements were made below 1 K, where they found relatively big events and only above a certain field threshold. Although size distributions are not presented in this work, the observations suggest that in this case the avalanches were thermally driven, i.e., they were flux jumps.

Stoddart et al. (1993) did similar experiments with slightly smaller Hall probes on 0.2 μm thick films of Pb, and later also on Nb films (Stoddart et al., 1995). Here, big avalanches were observed even in the beginning of the field sweep (ramp rate unknown), but again size distributions were not measured, thus preventing a comparison with SOC. However, from data obtained using a linear array of 4 micro-Hall probes, the authors could determine the in-plane correlations of the avalanche behavior. This analysis identified an average flux bundle radius of $R_c \approx 3.4\ \mu m$ for Nb at $T = 4.5$ K, in good agreement with the collective pinning theory.

Zieve et al. (1996) continued Hall-probe studies of avalanches in YBaCuO crystals, again performed at very low temperatures, even well below 1 K. Now the avalanche size statistics was reported, as well as hysteresis effects observed when the external field was cycled between 0 and 75 kOe. It was observed that the steps signaling avalanche behavior have a distinct onset field, H_{up}, during ascent, and that they disappear on the descending branch at a much lower field. Since H_{up} is found to be essentially independent of the field ramp rate, Zieve et al. (1996) exclude the case that the events are thermally driven. The avalanche size distributions turn out not to have power-laws, but to be instead sharply peaked around large size (750 vortices) events, which is indicative of flux jumping, and which is definitely not consistent

[3] Detailed experiments in by Heiden and Rochlin (1968) already suggested these kind of limitations in the pick up coil setup.

with the SOC. Nevertheless, Zieve et al. (1996) argue that their avalanches are dynamically driven, and that a sandpile analogy serves to explain the observed hysteretic behavior: It is not equivalent to add grains to a pile (to increase the field) or to remove grains from its base (to decrease the field), because the overall weight of the pile is supported mainly by the grains at lower positions. To account for the peaked size distributions the authors extend the analogy. In their opinion, vortex mass renormalization (Blatter et al., 1994) takes place at the very low temperatures of these experiments, making vortex inertial effects significant – and closer to some sandpile experiments, which show periodic avalanche events (Held et al., 1990; Rosendahl et al., 1993).

While SOC behavior was clearly not found in the experiments of Zieve et al., it is not equally obvious that their explanation is fully germane: it is today believed that inertial effects are negligible even at these low temperatures (Vinokur, 2001). An alternative explanation is provided by Pla et al. (1996) and others (Olson et al., 1997a), whose MD simulations suggest that broad pinning centers with low density – as expected for the samples measured by Zieve et al. (1996) – produce peaked distributions of avalanches, while sharp and dense pinning – as expected for the samples measured by Field et al. – produces distributions closer to a power law.

Returning to low-T_c materials, Nowak et al. (1997) studied avalanches in Nb films of thickness $d = 500$ nm. Their samples had an annular shape, with inner and outer diameters of 15 μm and 0.1 mm, respectively. Two 3×5 μm^2-sized Hall probes were used, one mounted over the central hole, and one at a position 22 μm off-center, allowing detection of the total flux involved in avalanches crossing the inner edge of the ring (center probe), and the local avalanche activity in the interior of the sample (off-center probe). Fig. 5 contains the main results of Nowak et al., where the upper two panels show how the local field varies as the applied field is cycled between ±500 G. The loops, obtained at different temperatures $t = T/T_c$, both contain distinct steps, and it is also evident that the magnitude and frequency of these avalanche events depend strongly on temperature. Moreover, by comparing the curves from the two probes (thick and thin line represent the center and internal probe, respectively), one finds them not always correlated, showing that both global and local flux avalanches indeed take place. The temperature dependence of this behavior is compiled in the lower part of the figure, where the main graph is a scatter plot over all the events detected by the center probe during two field cycles at each temperature. One sees that in a narrow range $0.3 < t < 0.4$ the distribution of avalanche sizes is broad and covers 1-2 decades. At lower temperatures $0.2 < t < 0.3$ the events cluster at large system-spanning sizes, typical for thermally triggered jumps[4], and interestingly one finds at even lower t that the sizes again become broadly distributed. At $t > 0.4$ only small avalanches occur, and the size distribution is monotonous and fits a decreasing exponential, as reported also earlier in (Heiden and Rochlin, 1998). From the figure insets, one sees that a power law $\sim s^{-2}$ describes the distribution at $t = 0.34$. In this work, also the ramp rate dependence of the avalanche activity was explored. In their range of rates, from 2 mOe/s to 20 Oe/s, the behavior remained unaffected, showing that the system is in the slowly driven regime.

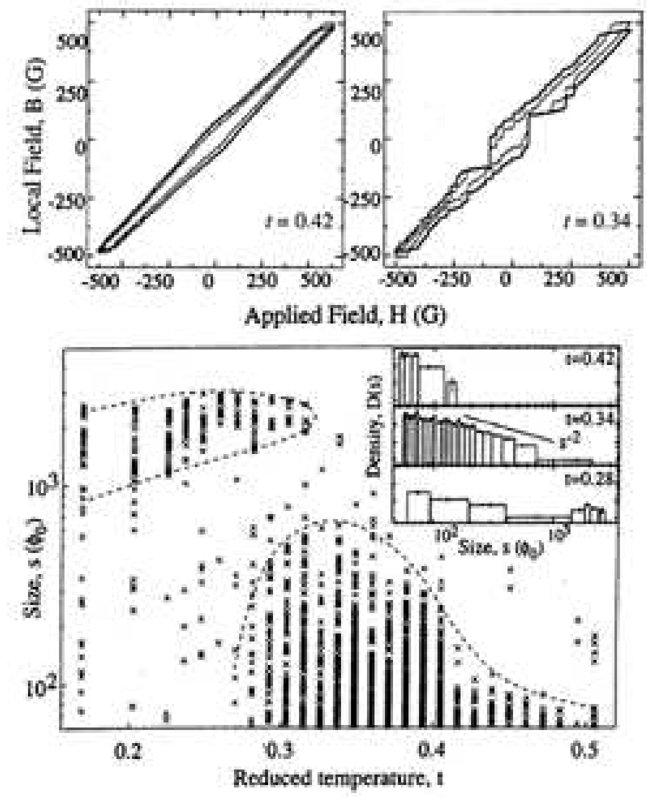

FIG. 5 Vortex avalanches reported by Nowak et al. (1997). Upper panels; local field vs. applied field for two normalized temperatures defined as $t = T/T_c$ (note the similarity with Fig. 1c). Lower panel; avalanche size vs. temperature diagram, and avalanche size distributions for different temperatures (inset).

Nowak et al. (1997) explain these data on the basis of a thermally triggered mechanism. The analysis makes quantitative use of the stability parameter β, and both the superconducting film and the substrate are assumed to absorb heat. For the particular sample in this study one has unstable conditions from the lowest temperatures

[4] This situation was also found in thin Nb films, although avalanche size statistics were not reported (Esquinazi et al., 1999).

as well as up to t = 0.37, which is fully consistent with the numerous large-s events in this range, as well as the rapid cut-off of large avalanches at higher t. The broad distribution of avalanches observed in the neighborhood of t = 0.37 is related to becoming marginally greater than 1. Such a fine tuning of parameters may evidently give power-law behavior, at least over a size range of one decade or so. An alternative explanation for these findings is given by Olson et al. (1997) based on MD simulations. These authors suggest that, at low temperatures, pinning is so strong that interstitial motion of vortices takes place, resulting in peaked distributions of avalanche sizes. At higher temperatures the pinning decreases, so "pin-to-pin" vortex flow is allowed, giving rise to wide distributions of avalanche size closer to a power law.

While the ring configuration of Nowak et al. appears elegant, it should be emphasized that the critical state in thin films placed in a perpendicular applied field deviates quite dramatically from the picture drawn in Fig. 1. In particular, for a ring-shaped superconductor, the central hole will contain a sizable non-uniform field due to shielding currents induced near the inner edge (Brandt, 1997). Actually, as the applied field is ramped from zero, there will be two flux fronts – one from each edge – advancing into the ring. The penetration from the inner edge consists of anti-vortices, because the edge field is here opposite to the applied field. As the field increases the two fronts eventually meet (for the Nowak et al. geometry this occurs at 3 m from the inner edge) and annihilation of the two vortex species takes place. We find that the actual field when this occurs is $H_c \simeq J_c d \simeq 150$ G, if we assume a value of $J_c = 2 \quad 10^6$ A/cm^2 for the Nb film. It is clear that the sample of Nowak et al. was cycled through a set of magnetized states with quite complicated flux distributions, where the purely geometrical (or demagnetization) effects may prevent drawing direct analogies to sandpile dynamics.

The first spatial-temporal study of internal vortex avalanches was made by Behnia et al. (2000), who made their measurements on a 20 m thick foil of Nb cut as a square with sides of length 0.8 mm. Unlike previous studies, these authors even explored the whole H T region between H_{c1} and H_{c2} (see Fig. 6(a)). At low temperatures, indicated by the hatched area, they found catastrophic, flux jump-like avalanches. Outside this region the behavior was qualitatively different, as exemplified by the results of the following experiment made at 4.8 K with an applied field around 1.5 kOe (see the circle in the phase diagram).

A 0.35 mm long Hall probe array consisting of 8 equally spaced 20 5 m^2 probes, each one with a sensitivity of 0.16 $_0$, was mounted on the sample along a mid-normal to one of the sides. After checking that the field creates a Bean model flux density profile { something that was difficult to assess in previous experiments due to the small numbers of Hall sensors { Behnia and coworkers made a series of measurements as the field was in-

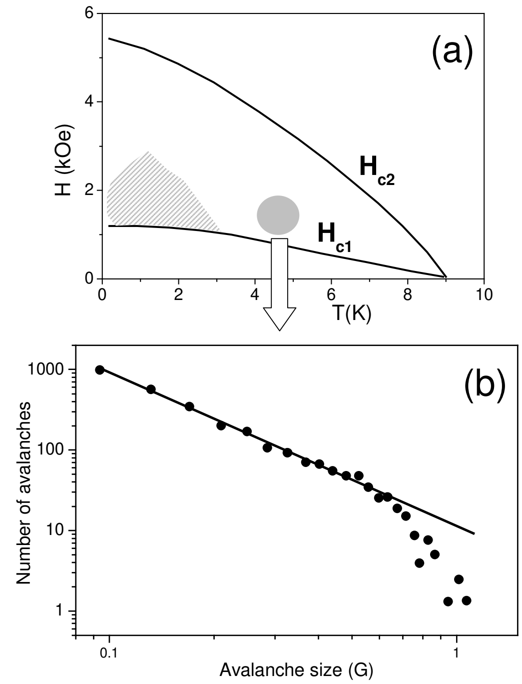

FIG. 6 Vortex avalanches reported by Behnia et al. (2000). (a) Catastrophic avalanches take place in the dashed area of the H T diagram, while small ones occur in the rest of the region between the two lines. (b) Typical avalanche size distribution corresponding to the small-avalanche region indicated by the gray circle in the H-T diagram.

creased from 1.5 kOe at the rate of 1.1 Oe/s. From each probe, they found a local field varying in steps, much like those reported by Nowak et al. (1997). The avalanche size statistics obtained by analyzing the signal from one probe is shown in Fig. 6(b). In the small-event region the size distribution follows a power-law with an exponent of -2.1 (fitted line), which is within the range of exponent values reported by Field et al. (1995). Deviations from the straight line start around 0.6 G, and reflect a clear deficiency of large size events. Note that the largest avalanche event is a field step of 1.1 G, corresponding to a sudden entry of 5 vortices under a probe area already populated by more than 6000 vortices. The authors leave the lack of big avalanches an open question. Could failure to wait for the extremely rare events be the simple explanation?

Behnia and coworkers investigated also the temporal correlations of avalanches by comparing the signal from Hall probes located a distance 50 m from each other. They estimated an average transit time of 0.8 ms, which gives an avalanche speed of a few cm/s. This can be compared with the velocity of vortex motion during flux flow, given by $v \quad _n J_c = _0 H_{c2}$, where $_n$ is the normal state resistivity. This gives velocities in the range of 25-8000 cm/s for parameters near the measuring conditions of Behnia et al. (2000). Since thermal activation and a possible current dependence of the resistivity would decrease this estimate, we conclude that the velocities of these avalanches, which have a broad size distribution, are consistent with a simple picture of the vortex motion, and in strong contrast to the ultra-fast dendritic ux penetration discussed later (in Section C).

Pushing the Hall probe technique even further, James et al. (2000) used a high resolution SHM to look at ux penetration into a 1 m thick Nb lm shaped as a 100 m wide strip. As the applied eld was slowly swept up and then down, they found (by keeping the sensor stationary 25 m from the edge) a step-like behavior in the Hall signal, much as in previous observations. But new aspects of the behavior were uncovered when the probe was scanned across a large part of the sample area. This showed that the ux does not penetrate with a smooth advancing front, but instead as a series irregularly shaped protrusions. These protrusions were easily distinguished from the much larger and blob-shaped ux patterns that sometimes form abruptly during eld sweeps at temperatures below 4 K. Whereas the blobs are rmly believed to be the visible result of conventional ux jumps, James et al. speculate about the origin of the numerous protrusions, which are apparent at all temperatures up to T_c. A key observation is that when the protrusions invade the ux free Meissner region the neighboring \ ngers" show a strong tendency to avoid each other. Had the protrusions been the ngerprint of scratches or other defects facilitating easy ux penetration in the lm, this kind of behavior would be very unlikely. Instead, James et al. suggest that some long-range repulsive force plays a role here, and indeed such an interaction does exist between vortices in thin samples. In contrast to the exponential dependence in bulk, there is for thin superconductors in a perpendicular eld a long-range inverse distance squared decay of the vortex-vortex force due to their surface screening currents (Pearl, 1964). Therefore, it may well be that the ux penetration in the form of these protrusions is an example of a dynamically driven vortex system full of avalanche dynamics. By taking di erences of the penetration pattern at two elds di ering by 10 G, it was demonstrated that the ux front advances by an apparently random sequence of localized bursts of ux motion. The size of these events was found to vary, but James et al. (2000) do not report quantitative size statistics of any kind.

So far, all the mentioned studies of vortex avalanches and their statistics, i.e., those where SOC ideas were examined using micro-Hall probes, have lacked knowledge about the actual \magnetic landscape" in which the probes were located. Furthermore, the number of recorded avalanches have been fairly limited, estimated to be around 150 events in the experiments of Zieve et al. (1996) and 5000 events in those of Behnia et al. (2000), and thus hardly su cient to convincingly establish power laws when broad size distributions are found. Both these shortcomings were largely improved by Altshuler and coworkers (Altshuler et al., 2002) who combined MOI with the recording of many long series of Hall

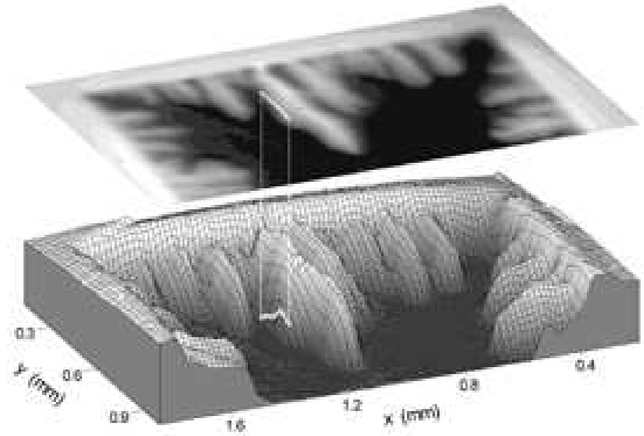

FIG. 7 Magnetic landscape in a Nb foil where an array of micro-Hall probes (white dots) detect avalanches coming down the slope of the largest \ ux ridge" (Altshuler et al., 2002).

probe data. Also the sample used was a Nb foil, 30 m thick and cut into a square with 1.5 mm sides. Figure 7 shows an MOI picture of ux penetration into the sample, and reveals that the distribution does not correspond to a simple sample-spanning critical state, but rather to a set of ux ridges, each having an \inverted-V," Bean's-like pro le. In this landscape an 11 probe Hall array, with 10 10 m^2 sensor areas, was mounted on the slope of the largest ridge, as indicated by the set of white dots [5] in Fig. 7.

Shown in Fig. 8 is the signal from one of the Hall sensors recorded as the eld was ramped from 0 to 3.5 kOe at 1 Oe/s and $T = 4.8$ K. When the curve is examined in detail (see lower inset), one nds clear signatures of avalanche dynamics along the whole range of elds. By analyzing the data from all of the 11 probes for repeated numbers of experiments made under the same conditions, several hundred thousand events were registered and analyzed. The resulting size distribution is plotted in the upper inset of the gure, which shows that the avalanche sizes covering two decades follow a power law with a slope of 3.0 0.2. To check the robustness of this result, the authors explored the avalanche behavior at many locations by remounting the Hall array at various positions in the landscape. A power law behavior was found everywhere and the exponent was essentially the same. The observed robustness gives grounds for the claim to have, for the rst time, observed SOC in ux dynamics.

In an attempt to investigate also the rigidity of the vortices involved in these avalanches, a pair of Hall arrays

[5] MOI experiments were recently made by the authors (speci cally for this Colloquium) on Nb foils kindly provided by K. Behnia. It was found that for samples similar to the ones studied in (Behnia et al., 2000) the ux penetration is globally non-Bean-like and quite similar to the one seen in Fig. 7, at least below 500 Oe.

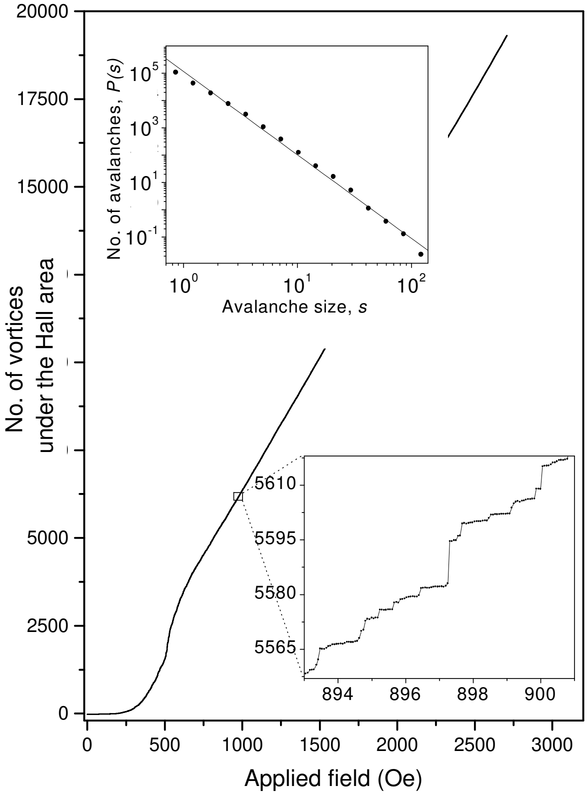

FIG. 8 Vortex avalanches reported by Altshuler et al. (2002). Main curve and lower inset: evolution of the number of vortices under the Hall probe areas seen in Fig. 7 as the external field is increased. Upper panel: resulting avalanche size distribution.

were mounted on the two sides of the Nb foil with the probes directly facing each other (Altshuler et al., 2002). The analysis of cross-correlations in these data indeed shows some degree of correlated behavior on the two sides of the sample, which is most clearly seen for the bigger avalanches.

Very recently, Radovan and Zieve (2003) used a micro Hall probe of 400 μm^2 area to look at the avalanche behavior in type II, Pb thin films of 100 nm thickness. The external field was slowly ramped up to 400 Oe, at various temperatures between 0.27 and 5.9 K. The authors found large avalanches at relatively high temperatures, and "micro-avalanches" at lower temperatures. Based on these observations they report power law distributions of avalanche sizes at the two temperatures 0.3 K and 4.3 K, with exponents of 2.0 and 1.1, respectively.

Another three recent papers report avalanches observed by micro Hall probes, although without including avalanche size statistics. Shung et al. (1998) found non-catastrophic vortex avalanches on a single crystal torus made from the heavy fermion superconductor UPt_3. The authors suggest that the observed sharp temperature onset for the appearance of avalanches is an indication of broken time reversal symmetry. Ooi et al. found signs of SOC in the $1/f$ noise spectrum they obtained from the analysis of avalanches found in $Bi_2Sr_2CaCu_2O_8$ single crystals[6]. The same kind of samples were studied also by Milner (2001), who below 1 K and up to 17 T found huge avalanches that strongly resemble those reported by Zieve et al. for YBCO crystals. Milner proposes a number of possible explanations to the phenomenon, ranging from domain structures that modulate the interplay between interpin and intervortex spacings, to broken time reversal symmetry in his samples.

C. Magneto-Optical Imaging experiments

The use of the space- and time-resolving power of MOI to study flux motion was pioneered already in the 1960s. Inspired by the visualization work of DeSorbo and Newhouse (1962), Wertheimer and Gilchrist (1967) used a fast camera technique to study how flux penetrates into disks of Nb, V and various alloy superconductors. As the applied field increased, they found events of abrupt flux invasion starting from a point along the perimeter. For the understanding of the nature of these avalanches, one particular observation was crucial, namely, that the events were accompanied by bubbles formed in the liquid coolant right above the sample surface. It was evident that thermo-magnetic flux jumps had, for the first time, been directly visualized. These early experiments showed also that the bursts of flux motion fall into two categories: "smooth" and "irregular" (or branching), referring to the geometrical shape of the invading flux front. The two types of avalanches were by Wertheimer and Gilchrist (1967) found to be related to the sample quality: smooth jumps were typical for "pure" samples, while the branching patterns were seen only in the alloy disks, suggesting that material inhomogeneities drastically perturb the course of the avalanches.

Then in 1993, the branching scenario of flux penetration was revisited by Leiderer et al. (1993) making full use of the high spatial and temporal resolution offered by the ferrite garnet indicator films. A typical pattern, this time observed in thin films of YBaCuO, is shown in Fig. 9(a). These magnificant dendritic patterns were triggered by perturbing a flux-filled remnant state with a laser pulse fired at a point near the sample edge. This heated spot became the root of the branching structure, which is where the trapped flux has escaped the sample. The study revealed that if the experiments were repeated in exact detail, the branching forms would nevertheless vary widely. In other words, these events produce "irregular" flux patterns that are not controlled by quenched disorder in the sample.

Soon after, Duran et al. (1995) found essentially the same spectacular behavior in films of Nb. This time the

[6] These experiments cannot be easily compared to others presented in this Colloquium, since they do not involve a slow increase of the applied field at a fixed temperature.

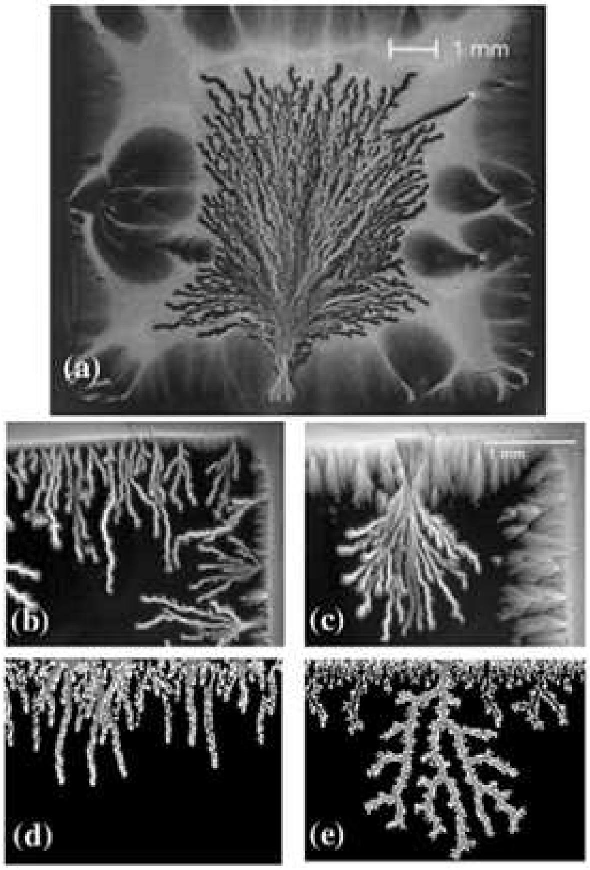

FIG. 9 Flux dendrites formed abruptly in thin film superconductors. (a): In YBaCuO at $T = 4.2$ K; (b) and (c): In MgB_2 at $T = 3.8$ and 10 K, respectively; (d) and (e): By vortex dynamics simulations made for low and high temperature (see text).

dendritic flux patterns were produced by simply lowering the field from 135 Oe applied during the sample's initial cooling to various temperatures below T_c. These films were 500 nm thick, and the overall conditions resemble closely the descending field branch in the Hall probe experiments of Nowak et al.. What the MOI revealed was that the dendritic patterns actually vary in their morphology, changing from quasi-1D structures at temperatures below 0.35 T_c, to highly branched structures a la the one seen in Fig. 9(a) at temperatures approaching 0.65 T_c. These findings strongly suggest that the cluster of large-size events at the lowest temperatures reported by Nowak et al. (1997) are due to the abrupt formation of such macroscopic dendritic structures.

Dendritic avalanches with the same qualitative characteristics were observed quite recently also in films of MgB_2 (Johansen et al., 2002), and Nb_3Sn (Rudnev et al., 2003) only here, as in the very early MOI experiments, the abrupt events were triggered simply by ramping up the applied field. During slow ramps after zero-field-cooling to 4 K, the films became invaded by numerous dendrites, which burst into the Meissner state region one at a time (see Fig. 9(b)). for the case of MgB_2. Near 10 K, the dendritic structures become much larger, as in (c), whereas at even higher temperatures and up to $T_c = 39$ K such "irregular" features cease to be formed. What is the nature of this type of avalanches, and why do they take the form of branching flux dendrites? To find the answer, one should note from Fig. 9 that the dendrite fingers have a strong tendency to avoid overlapping. As discussed in relation to the work of James et al. (2000), this is probably a result of the long-range action of the repulsive force between vortices in thin films. The same "explosive" force can possibly also be responsible for the branching itself, although the mechanism for selecting these seemingly random bifurcation points is not yet clear.

These observations formed the basis for a MD-type of computer code Johansen et al. (2002), where the dynamical equation (2) was modified to account for the thin film geometry, i.e., by using $1/r^2$ intervortex forces, and adding a term for the Lorentz force from the Meissner currents, which in thin superconductors flow over the whole area. Finally, a thermal component was introduced: When any vortex i moves a distance Δr_i, given by evaluating v_i, an amount of heat, $\Delta Q_i = \Delta r_i f_i$, is produced that raises the temperature in the neighborhood of the trajectory by $\Delta T \propto \Delta Q_i$. This has then a direct effect on the local pinning conditions, since the pinning force is taken to be T-dependent (as $f_i^{vp} \propto 1 - T/T_c$). Results of these simulations are seen in Figs. 9(d) and (e), showing flux penetration patterns corresponding to low and high temperatures, respectively. Notice that some of the dendritic fingers have a "spine," which is the instantaneous map of the temperature rise due to recent traffic of vortices penetrating from the upper edge. Evidently, the avalanche morphology found experimentally is very well reproduced by these simulations. Also analytical efforts have addressed the same question, and calculations by Aranson et al. (2001) suggest that vortex "micro-avalanches" can be triggered by a hot spot, and that the temperature distribution can evolve in a branching manner. Despite the qualitative success of the theoretical work, more needs to be done to understand these avalanches at a quantitative level. For example, MOI using double-pulse laser illumination with time intervals less than 10 ns has shown that the speed of dendrite propagation in YBaCuO is close to 25 km/s (Bolz, 2002). This is orders of magnitude higher than the avalanche velocity reported by Behnia et al. (2000), and actually the two scenarios appear totally different, as one would expect for dynamically and thermally driven systems. Interestingly, the speed of dendrite propagation even exceeds the sound velocity in the material, raising questions about which non-phonon heat conduction mechanism is here active.

Very recently, MOI was used to study also non-catastrophic avalanches. In the work of Bobyl et al. (2003) the first spatially resolved observation of vortex avalanches on a mesoscopic scale is reported. A thin film of MgB_2 was investigated at temperatures below

10 K, where flux dendrites can form in this material, but the applied field was now kept below the threshold for dendrite formation. By increasing the field slowly (60 mOe/s) avalanches were observed by subtracting subsequent images recorded at intervals of $\Delta H = 0.1$ Oe. All the avalanches were seen to have a regular shape with no sign of ramification, and they appear at seemingly random places mainly near the edge of the film. The total number of vortices participating in an avalanche varied between 50 and 10000. However, the work does not report any detailed statistics. Interestingly, the mesoscopic avalanches, having a typical linear size of 10-20 μm, continue to form also at the higher fields where the large dendrites dominate the flux penetration. Moreover, it is found that, above 10 K, both types of avalanches (mesoscopic ones and dendrites) cease to form suggesting that only one physical mechanism is responsible for both.

In a work by Aegerter et al. (2003) an 80 nm thick film of YBaCuO was, after zero-field cooling to 4.2 K, subjected to a perpendicular field slowly increased in a stepwise manner. After each field step of 0.5 Oe, the sample was allowed to relax for 10 seconds before an image was taken. By subtracting subsequent images, the difference in flux density $\delta B_z(x,y)$ was obtained and integrated over a sub-area $L \times L$ of the total field of view. This revealed clearly that the evolution of the magnetic flux inside the sample is intermittent with occasional bursts of various sizes. To allow for a finite-size scaling type of analysis, the authors let L vary between 180 μm and 15 μm. The histogram of avalanche size distributions with 4 different L values shows power laws, which when combined extend over more than 3 decades. Furthermore, plotting the histogram versus the scaled avalanche size s/L^D shows a good data collapse using $\tau = 1.29$ and $D = 1.89$. In addition, the authors measure both the so-called roughness exponent and the fractal dimension of the avalanche clusters, and show that the set of exponents obey a universal scaling relation. This gives strong indication that SOC is present in their system.

Related to this is the earlier observation of kinetic "roughening" of advancing flux fronts in high-T_c films (Surdeanu et al., 1999). By applying scaling analysis, it was shown that there exists two regimes; at small length scales or short time scales, where static disorder dominates, the roughening and growth exponents correspond to a directed-percolation-depinning model, whereas at larger scales temporal stochastic noise dominates and the exponents come close to those of the Kardar-Parisi-Zhang (KPZ) model. This finding has common ground with finding of the dynamically driven avalanche community: theoretical models in sandpiles have established relations between the critical exponents of avalanche dynamics and those for interface growth, including for the KPZ (Chen and Nijs, 2002; Paczuski and Bassler, 2000).

The MOI technique made a giant leap forward when Goa et al. (2002) succeeded to resolve individual vortices, and thereby directly visualizing their motion. Immediately, one obtained here a new method capable of

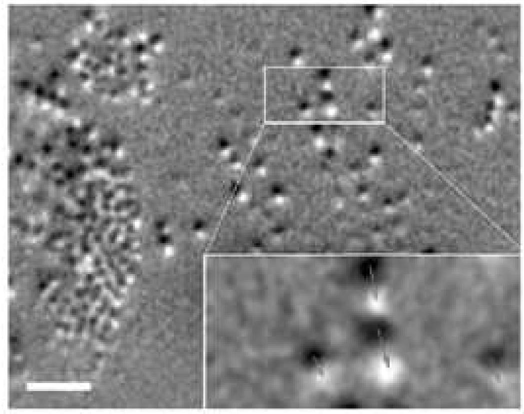

FIG. 10 Vortex avalanches in $NbSe_2$ observed by MOI. The bright and dark dots show where vortices have moved to and from, respectively, during a field step of 4 mOe. The scale bar is 10 micron long.

following vortex avalanche dynamics in full detail,[7] and not only through sampling of the flux density integrated over some area. In particular, single-vortex resolution MOI could contribute to test experimentally the role of interstitial versus "pin-to-pin" motion of vortices during avalanches, as predicted in MD simulations (Olson et al., 1997,a), or even the details of "braided rivers" of vortices resulting from CA simulations (Bassler et al., 1999). To illustrate what is now possible, Fig. 10 shows an image which is the difference of two MOI pictures recorded before and after the applied field was increased by 4 mOe during 1 second. The superconductor is here a 0.1 mm thick single crystal of $NbSe_2$ at 4 K. The bright and dark dots show the local increase and decrease of the field, i.e., they are the positions the vortices have hopped to and from, respectively. The areas where such dots are absent also contain vortices, but they have not moved during this particular interval. From the image one can clearly identify vortex avalanches of various sizes, e.g., there is a quite large event taking place on the left side, and many small ones, down to individual hops, are scattered over the whole field of view. Although this new high-resolution MOI method has not yet been used specifically to study avalanche aspects, it is evident that the experimental potential is huge, and will bring us closer to a full understanding of vortex dynamics.

D. Miscellaneous experiments

Vortex avalanches not associated with conventional flux jumps have been detected also through other

[7] Compared to Lorentz microscopy, the only other method with the same capability, the MOI is not restricted to samples so thin that the electron beam goes through.

TABLE I List of experiments reporting vortex avalanche size distributions. The information in the table was extracted directly or indirectly from the references cited. "Exp," "peak," "power" (exponent) and "stexp" refer to exponential, peaked, power-law and stretched exponential distributions of avalanche sizes, respectively.

Ref	Geom :	Material	Sensor	Avalanche type	T/T_c	H range [kOe]	Rate [Oe/s]	Avalanche distribution
Heiden et al. (1968)	hollow cylinder	Pb-In	pickup coil	off-edge	0.6	0.55 – 0.85	10 – 100	exp
Field et al. (1995)	hollow cylinder	Nb-Ti	pickup coil	off-edge	0.3	2.25 – 7.55	5	power(1.4 – 2.2) (slow ramps)
Zieve et al. (1996)	planar	YBCuO crystal	Hall probe	internal	0.01	0 – 80	7	peak
Nowak et al. (1997)	planar ring	Nb film	Hall probes	off-edge & internal	0.15 – 1.12	0.5 – 0.5	0.002 – 20	peak/power(2.0)
Aegerter (1998)	planar	BSCCO crystal	SQUID	off-edge	0.06 – 0.8	?	0	exp/power(2)
Behnia et al. (2000)	planar	Nb film	Hall probes	internal	0.52	1.5	1	peak/power(2.05) /stexp
Altshuler et al. (2002)	planar	Nb foil	Hall probes & MOI	internal	0.5	0 – 3.5	1	power(3.0)
Aegerter et al. (2003)	planar	YBCO film	MOI	internal	0.05	0-0.15	0.05	power(1.30)
Radovan, Zieve (2003)	planar	Pb film	Hall probes	internal	0.7	0-0.04	0.2-3.3	peak /power(1.1,2.0)

techniques like SQUID Magnetometry (Aegerter, 1998; Kopelevich and Moehlecke, 1999; Wang and Shi, 1993) and torque magnetometry (Hope et al., 1999). Among them, only Aegerter (1998) reported avalanche size distributions by studying the detailed flux motion during creep in a $Bi_2Sr_2CaCu_2O_8$ crystal. Instead of driving the vortices by increasing the applied magnetic field, the avalanches were here created by thermal activation in a constant applied field. Using a SQUID sensor the events were recorded as time went by for more than 10^5 seconds. The main finding is that at low temperatures (0.06 T_c) the distribution of avalanche sizes shows power law behavior, whereas at higher temperatures (0.8 T_c) the distribution becomes exponential. A theoretical discussion of these results has been provided by Mulet et al. (2001), based on the Bassler-Paczuski CA with additional Monte-Carlo rules to account for the slow thermal activation. They conclude that the critical exponents obtained in creep experiments can be related to, but are not identical to, those predicted in the original SOC scheme.

To summarize, Table 1 gives an overview of the main results concerning avalanche statistics and experimental conditions reported in all the papers reviewed in this Colloquium.

V. SUMMARY AND OPEN QUESTIONS

When an account of a given scientific subfield is written long after the key developements, a mysterious filtering process takes place which results in a nice concerto of experiments, perfectly aimed at the "big question." However, in the case of vortex avalanche experiments cruel reality has forced us to replace such an idyllic approach by a much more disjointed literary style. Nevertheless, we have still been able to distill from the available experiments a set of issues and questions that may contribute significantly to the understanding of the physics beyond vortex avalanches.

Although low-T_c materials dominate most of the experiments in which avalanche size statistics are reported, the types of samples used are widely different (cylinders, films, foils) and the temperature, field ranges, and field sweep rates vary quite a bit from report to report. The occurrence of avalanches in the different regions of the H – T phase diagram has been only rarely explored. In practice, it has proved difficult to tell if the observed avalanches are thermally or dynamically triggered, although there is consensus that the first ones abound at T below 4 K or so – at least in low-T_c samples. Remarkably, only one experimental work on high-T_c materials reports to have found non-catastrophic avalanches during slowly increasing field. Is this general situation due to lack of instrumental resolution, or perhaps are the avalanches just "smoothed out" by thermal activation?

Even when non-catastrophic avalanches are detected as the field is swept, opinions are divided as to their origin. Some authors claim that Self Organized Criticality is at the core of the dynamics. But robust, well-defined power laws have proved somewhat elusive: Nature does not seem to like more than two decades of avalanche sizes measured in a single experiment...or have we failed to be patient enough to collect the appropriate wealth of data (Avnir et al., 1998)?

Some simulations suggest that the type of avalanche size distribution may depend on the nature and density of pinning sites – in analogy with experiments in sandpiles with different types of grains and bases on which the piles are grown. Definitive experiments to check this hypothesis can be performed only on samples with artificially tailored pinning landscapes. If true, could measurements of avalanche size distributions become a tool to figure out the pinning features of a given sample?

In the case of non-catastrophic events, and when power law behavior is found, there is a great dispersion in the critical exponent of the avalanche size distributions. This applies to both experiment and theory: While for the first category the exponent ranges from 1.3 to 3.0, in the second it typically spans from 1 to 2, and it can go even further. An important principle question then arises: Is it possible to establish a one-to-one correspondence between the different experiments and models?

Power law distributions of avalanche sizes are expectedly associated to linear flux profiles (like originally proposed by Bean), since nonlinear ones, in principle, cannot result in scale-invariant avalanches. Many of the recent experiments have been made on thin superconductors in a perpendicular magnetic field where the flux density profiles have an enhanced slope near the sample's edge and center. This applies even for samples with a constant critical current density. In bulk samples there is also a possibility for having non-linear profiles due to a B-dependence of the critical current density, e.g. as in the Kim model. What exactly are the differences in avalanche behaviors when non-Bean flux profiles are present? Are they diminished when the sensors cover only a small area of the sample?

The very nature of the "avalanching objects" is sometimes in question due to the lack of appropriate instruments: are they individual vortices, or flux bundles? Are they rigid entities? Or perhaps we are seeing the irregular growth of tiny flux fingers, only visible with the most sophisticated instruments?

Imaging techniques suggest that the scenario where avalanches take place can eventually be quite distant from the basic Bean's critical state. Catastrophic avalanches seem to be associated with "bursting," non-repeatible dendritic structures, while non-catastrophic ones are mostly found in materials where the field penetrates as fingers with a Bean's-like cross section. Even "roughness" in the critical state can be related to vortex avalanches, but this relation is just starting to be properly established. MOI seems to have the potential to materialize our wildest dreams in vortex avalanche studies: high spatial and temporal resolutions, and the ability to take "magnetic pictures" of an ample region of the sample. This technique is only limited by the speed of data acquisition and data storage capabilities...but, with a little patience, these will find their way from Hollywood special effects departments to scientific labs.

All in all, it becomes clear that there are more questions than answers in the field of vortex avalanches. This is of course good news for the scientists working in Complex Systems, but probably even better news for the vortex physics community, which is busy these days tightening up the last bolts to the equilibrium $H - T$ diagram of superconductors.

Acknowledgments

The authors acknowledge useful discussions with Ch. Aegerter, P. Bak, K. E. Bassler, A. J. Batista-Leyva, K. Behnia, E. H. Brandt, J. R. Clem, T. Giamarchi, A. Gurevich, H. Herrmann, H. Jaeger, H. J. Jensen, P. Leiderer, X. S. Ling, J. Luzuriaga, M. C. Marchetti, M. Marchevsky, R. Mulet, E. Nowak, M. Paczuski, G. Parisi, H. Pastoriza, O. Ramos, G. Reiter, B.U. Runge, G. Seidler, D. V. Shantsev, O. Sotolongo, V. Vinokur, R. J. Wijngaarden, Y. Yeshurun and E. Zeldov. We thank A. F. Olsen for MOI work made specifically for this paper. E. A. thanks A. Rivera, J. Altshuler and M. Alvarez for inspiration and support, and also the ACLS/SSRC Working Group on Cuba for online access to bibliographic materials. T. H. J. is grateful to his patient family, and for financial support from the Norwegian Research Council.

References

Abrikosov, A. A., 1957, Sov. Phys. JETP 5, 1174.

Aegerter, C. M., 1998, Phys. Rev. E 58, 1438.

Aegerter, C. M., M. S. Welling, R. J. Wijngaarden, 2003, eprint cond-mat/0305591.

Altshuler, E., O. Ramos, C. Martinez, L. E. Flores, C. Noda, 1999, Phys. Rev. Lett. 86, 5490.

Altshuler, E., 2001, Some Contemporary Problems in Condensed Matter Physics, edited by S.J.Vlaev, L.M. Gaggero-Sager and V. Droeglazov, Contemporary Fundamental Physics (Nova Science Publishers, Inc., Commack, NY).

Altshuler, E., T. H. Johansen, Y. Paltiel, P. Jin, O. Ramos, K. E. Bassler, G. Reiter, E. Zeldov, C. W. Chu, 2002, eprint cond-mat/0208266.

Aranson, I., A. Gurevich, V. Vinokur, 2001, Phys. Rev. Lett. 87, 067003.

Avnir, D., O. Biham, D. Lidar, O. Malcai, 1998, Science 279, 39.

Bak, P., C. Tang, K. Wiesenfeld, 1987, Phys. Rev. Lett. 77, 111.

Bak, P., 1996, How Nature Works{The Science of Self-Organized Criticality (Copernicus, NY).

Barford, W., W. H. Bee, M. Steer, 1993, J. Phys. Cond. Matter 5, L333.

Barford, W., 2002, Phys. Rev. B 56, 425.

Barone, A., G. Paterno, 1982, Physics and the Applications of the Josephson E ect (Academic Press, NY).

Bassler, K. E., M. Paczuski, 1998, Phys. Rev. Lett. 81, 3761.

Bassler, K. E., M. Paczuski, G. Reiter, 1999, Phys. Rev. Lett. 83, 3956.

Bassler, K. E., M. Paczuski, E. Altshuler, 2001, Phys. Rev. B 64, 224517.

Bean, C. P., 1964, Phys. Rev. Lett. 8, 250.

Behnia, K., C. Capan, D. Mailly, B. Etienne, 2000, Phys. Rev. B 61, 3815.

Bending, S. J., 1999, Adv. Phys. 48, 449.

Blatter, G., V. B. Geshkenbein, V. M. Vinokur, 1991, Phys. Rev. Lett. 66, 3297.

Blatter, G., M. V. Feigel'man, V. B. Geshkenbein, A. I. Larkin, V. M. Vinokur, 1994, Rev. Mod. Phys. 66, 1125.

Bobyl, A. V., D. V. Shantsev, Y. M. Galperin, A. F. Olsen, T. H. Johansen, W. N. Kang, S. I. Lee, 2003, eprint cond-mat/0304603.

Bolz, U., 2002, Magnetooptische Untersuchungen der Flussdynamik in YBaCuO-Filmen auf ultrakurzen Zeitskalen (PhD thesis, University of Konstanz, Germany).

Bonabeau, E., P. Lederer, 1995, Phys. Rev. B 52, 494.

Bonabeau, E., P. Lederer, 1996, Physica C 256, 365.

Brandt, E. H., 1997, Phys. Rev. B 55, 14513.

Bretz, M., J. B. Cunningham, P. L. Kurczynski, F. Nori, 1992, Phys. Rev. Lett. 69, 2431.

Campbell, A. M., J. E. Evetts, 1972, Adv. Phys. 21, 199.

Carlson, J. M., J. Doyle, 1999, Phys. Rev. E 60, 1412.

Chen, Ch., M. den. Nijs, 2002, Phys. Rev. E 66, 011306.

Christensen, K., A. Corral, V. Frette, J. Feder, T. J. J ssang, 1996, Phys. Rev. Lett. 77, 107.

Cruz, R., R. Mulet, E. Altshuler, 2000, Physica A 275, 15.

D'Anna, G., F. Nori, 2000, Phys. Rev. Lett. 85, 4096.

DeGennes, P. G., 1966, Superconductivity of Metals and Alloys (Benjamin, NY).

DeSorbo, W., V. L. Newhouse, 1962, J. Appl. Phys. 33, 1004.

Dingle, R., H. L. Stormer, A. C. Gossard, W. Wiegman, 1978, Appl. Phys. Lett. 33, 532.

Duran, C., P. L. Gammel, R. E. Miller, D. J. Bishop, 1995, Phys. Rev. B 52, 75.

Esquinazi, P., A. Setzer, D. Fuchs, Y. Kopelevich, C. Assman, 1999, Phys. Rev. B 60, 12454.

Field, S., J. Witt, F. Nori, W. S. Ling, 1995, Phys. Rev. Letters 74, 1206.

Field, S., N. Venturi, F. Nori, 1996, Phys. Rev. Lett. 74, 74.

Frette, V., K. Christensen, V. Malthe-S rensen, J. Feder, T. J ssang, P. Meakin, 1996, Nature 379, 49.

Gammel, P. L., U. Yaron, A. P. Ramirez, J. D. Bishop, A. M. Chang, R. Ruel, L. N Pfei er, E. Bucher, G. D'Anna, K. Mortensen, M. R. Eskildsen, P. H. Kes, 1998, Phys. Rev. Lett. 80, 833.

Goa, P. E., H. Hauglin, M. Baziljevich, E. Il'yashenko, P. L. Gammel, T. H. Johansen, 2001, Supercond. Sci. Technol. 14, 729.

Heiden, C., G. I. Rochlin, 1968, Phys. Rev. Lett. 21, 691.

Held, G. A., D. H. Solina, D. T. Keane, W. J. Haag, P. M. Horn, G. Grinstein, 1990, Phys. Rev. Lett. 65, 1120.

Hope, A. P., M. J. Naughton, D. A. Gajewski, M. B. Maple, 1999, Physica C 320, 147.

Huang, Y., G. Ouillon, H. Saleur, D. Sornette, 1997, Phys. Rev. E 55, 6433.

Jaeger, H., 2000, Private communication

James, S. S., S. B. Field, J. Siegel, H. Shtrikman, 2000, Physica C 332, 445.

Jensen, H. J., 1998, Self Organized Criticality- Emergent Complex Behaviour in Physical and Biological Systems (Cambridge University Press, Cambridge).

Johansen, T. H., M. Baziljevich, D. V. Shantsev, P. E. Goa, Y. M. Galperin, W. N. Kang, H. J. Kim, E. M. Choi, M.-S. Kim, S. I. Lee, 2001, Supercond. Sci. Technol. 14, 726.

Johansen, T. H., M. Baziljevich, D. V. Shantsev, P. E. Goa, Y. M. Galperin, W. N. Kang, H. J. Kim, E. M. Choi, M.-S. Kim, S. I. Lee, 2002, Europhys. Lett. 59, 599.

Kadano , L. P., S. R. Nagel, L. Wu, S. Zhou, 1989, Phys. Rev. A 39, 6524.

Kim, Y. B., C. F. Hempstead, A. Strnad, 1963, Phys. Rev. 131, 2486.

Koblischka, M. R., R. W. Wijngaarden, 1995, Supercond. Sci. Technol. 8, 199.

Kopelevich, Y., S. Moehlecke, 1998, Phys. Rev. B 58, 2834.

Larkin, A. I., Yu. N Ovchinnikov, 1973, Zh. Eksp. Teor. Fiz. 65, 1704.

Larkin, A. I., Yu. N Ovchinnikov, 1973, Zh. Eksp. Teor. Fiz. 34, 409.

Lee, T. S., N. Missert, L. T. Sagdahl, J. Clarke, J. R. Clem, K. Char, J. N. Ekstein, D. K. Fork, L. Lombardo, L. A. Kapitulnik, L. F. Schneemeyer, J. V. Waszczak, R. B. Van Dover, 1993, Phys. Rev. Lett. 74, 2796.

Leiderer, P., J. Boneberg, P. Brull, V. Bujok, S. Herminghaus, 1993, Phys. Rev. Lett. 71, 2646.

Milner, A., 2001, Physica C 294-295, 388.

Mints, R. G., A. L. Rakhmanov, 1981, Rev. Mod. Phys. 53, 551.

Mohler, G., D. Stroud, 1999, Phys. Rev. B 60, 9738.

Mulet, R., R. Cruz, E. Altshuler, 2001, Phys. Rev. B 63, 094501.

Newman, M. E. J., K. Sneppen, 1996, Phys. Rev. E 54, 6226.

Nowak, E. R., O. W. Taylor, L. Liu, H. M. Jaeger, T. J. Selinder, 1997, Phys. Rev. B 55, 11702.

O'Brien, K. P., M. B. Weissman, 1992, Phys. Rev. A 46, 4475.

Olson, C. J., C. Reichhardt, F. Nori, 1997, Phys. Rev. B 56, 6175.

Olson, C. J., C. Reichhardt, J. Groth, S. B. Field, F. Nori, 1997, Physica C 290, 89.

Ooi, S., T. Shibaushi, T. Tamegai, 2000, Physica C 284-288, 775.

Oral, A., S. J. Bending, M. Henini, 1996, Appl. Phys. Lett. 69, 1324.

Paczuski, M., K. E. Bassler 2000, Phys. Rev. E 62, 5347.

Pan, W., S. Doniach, 1994, Phys. Rev. B 49, 1192.

Pearl, J., 1964, Appl. Phys. Lett. 5, 65.

Pla, O., N. K. Wilkin, H. J. Jensen, 1996, Europhys. Lett. 33, 297.

Plourde, B., F. Nori, M. Bretz, 1993, Phys. Rev. Lett. 71, 2749.

Prozorov, R., D. Giller 1999, Phys. Rev. B 59, 14687.

Radovan, H. A., R. J. Zieve, 2003, eprint cond-mat/0307092.

Richardson, R. A., O. Pla, F. Nori, 1994, Phys. Rev. Lett. 72, 1268.

Rosendahl, J., M. Vekic, J. Kelley, 1993, Phys. Rev. E 47, 1401.

Rosendahl, J., M. Vekic, J. Rutledge, 1994, Phys. Rev. Lett.

73, 537.

Rudnev, I. A., S. V. Antonenko, D. V. Shantsev, T. H. Johansen, A. E. Primenko, 2003, Cryogenics. 43, 663.

Runge, B. U., U. Bolz, J. Eisenmenger, P. Leiderer, 2000, Physica C 341–348, 2029.

Schmidt, M. F., N. Israeloff, A. M. Goldman, 1996, Phys. Rev. Lett. 70, 2162.

Schwarz, J. M., D. S. Fisher, 2001, Phys. Rev. Lett. 87, 096107.

Seidler, G. T., C. S. Carrillo, T. F. Rosenbaum, U. Welp, G. W. Crabtree, V. M. Vinokur, 1993, Phys. Rev. Lett. 70, 2814.

Shung, E., T. F. Rosenbaum, M. Sigrist, 1998, Phys. Rev. Lett. 80, 1078.

Stoddart, S. T., S. J. Bending, A. K. Geim, M. Henini, 1993, Phys. Rev. Lett. 71, 3854.

Stoddart, S. T., S. J. Bending, A. K. Geim, M. Henini, 1995, Supercond. Sci. Technol. 8, 459.

Surdeanu, R., R. J. Wijngaarden, E. Visser, J. M. Huijbregtse, J. H. Rector, B. Dam, R. Griessen, 1999, Phys. Rev. Lett. 83, 2054.

Tang, C., 1993, Physica A 194, 315.

Thomson, W., 1884, in Lectures on Molecular Dynamics and the Wave Theory of Light (Johns Hopkins University, Baltimore).

Vinokur, V. M., M. V. Feigel'man, V. B. Geshkenbein, 1991, Phys. Rev. Lett. 67, 915.

Vinokur, V., 2001, Private communication.

Wang, Z., D. Shi, 1993, Phys. Rev. B 48, 9782.

Wertheimer, M. R., J. le G. Gilchrist, 1967, J. Phys. Chem. Solids 28, 2509.

Wischmeyer, C. R., 1967, Phys. Rev. 154, 323.

Yeshurun, Y., A. P. Malozemoff, A. Shaulov, 1996, Rev. Mod. Phys. 68, 911.

Zeldov, E., J. R. Clem, M. McElfresh, M. Darwin, 1994, Phys. Rev. B 49, 9802.

Zieve, R. J., T. F. Rosenbaum, H. Jaeger, G. T. Seidler, G. W. Crabtree, U. Welp, 1996, Phys. Rev. B 53, 11849.